Interventions can shift the thermal optimum for parasitic disease transmission

Karena H. Nguyen[a,1,2] , Philipp H. Boersch-Supan[b,c,d,1,2] , Rachel B. Hartman[a] , Sandra Y. Mendiola[a],
Valerie J. Harwood[e], David J. Civitello[a] , and Jason R. Rohr[f,g,h]

[a]Department of Biology, Emory University, Atlanta, GA 30322; [b]British Trust for Ornithology, Thetford, IP24 2PU, United Kingdom; [c]Emerging Pathogens Institute, University of Florida, Gainesville, FL 32610; [d]Department of Geography, University of Florida, Gainesville, FL 32611; [e]Department of Integrative Biology, University of South Florida, Tampa, FL 33620; [f]Department of Biological Sciences, University of Notre Dame, Notre Dame, IN 46556; [g]Eck Institute for Global Health, University of Notre Dame, Notre Dame, IN 46556; and [h]Environmental Change Initiative, University of Notre Dame, Notre Dame, IN 46556

ECOLOGY

Temperature constrains the transmission of many pathogens. Interventions that target temperature-sensitive life stages, such as vector control measures that kill intermediate hosts, could shift the thermal optimum of transmission, thereby altering seasonal disease dynamics and rendering interventions less effective at certain times of the year and with global climate change. To test these hypotheses, we integrated an epidemiological model of schistosomiasis with empirically determined temperature-dependent traits of the human parasite *Schistosoma mansoni* and its intermediate snail host (*Biomphalaria* spp.). We show that transmission risk peaks at 21.7 °C (T_{opt}), and simulated interventions targeting snails and free-living parasite larvae increased T_{opt} by up to 1.3 °C because intervention-related mortality overrode thermal constraints on transmission. This T_{opt} shift suggests that snail control is more effective at lower temperatures, and global climate change will increase schistosomiasis risk in regions that move closer to T_{opt}. Considering regional transmission phenologies and timing of interventions when local conditions approach T_{opt} will maximize human health outcomes.

temperature | climate change | snail control | epidemiological modeling | neglected tropical disease

Temperature is important to the transmission of most infectious diseases, but the effects of temperature variability on parasite and host traits and their interactive effects on infection dynamics are poorly understood across many host–parasite systems (1–3). The variable responses of host and parasite traits to altered thermal regimes (i.e., thermal trait variation) could also impact intervention efficacy if the mortality of temperature-sensitive life stages is greater than the relative contribution of natural, temperature-dependent constraints on parasite transmission. For example, anthelminthic drugs decrease parasite transmission but likely have little effect on temperature-dependent transmission dynamics because adult parasites are buffered from environmental temperature in endothermic hosts. In contrast, vector control measures and water sanitation cause vector and parasite mortality, respectively, that is independent of ecophysiological constraints and irrespective of environmental temperature (4–6).

If interventions override natural temperature-dependent constraints on transmission, they could cause shifts in the thermal optimum (T_{opt}) of parasite transmission, which could theoretically alter seasonal disease dynamics and render interventions less effective at certain times of the year and with global warming. This, in turn, would affect risk assessments and intervention planning for various disease systems (7, 8), especially under global climate change. Nevertheless, the hypotheses of intervention-related shifts to the T_{opt} of transmission and the resulting knock-on effects on disease phenology and intervention efficacy have never been proposed or tested.

Human schistosomiasis, which affects more than 200 million people worldwide, is a major source of human morbidity and mortality in sub-Saharan Africa (9) and represents an ideal system to test these hypotheses. *Schistosoma mansoni*, an important

causative parasite species, is transmitted through two aquatic larval stages (Fig. 1). Miracidia infect intermediate snail hosts (*Biomphalaria* spp.), and cercariae are released from snails to infect humans (10). Because free-living parasite larvae and snails are ectotherms, aquatic transmission is influenced by temperature (11, 12), with warm temperatures decreasing miracidial (13, 14) and cercarial survival (15) and reducing the odds of infection (13, 16). Although several *Schistosoma* parasite and snail traits are temperature-dependent (17–21), many models assume temperature-invariant transmission (12, 22, 23). Additionally, schistosomiasis interventions either target temperature-sensitive transmission stages, such as molluscicides, snail removal, and water sanitation, or temperature-insensitive stages, such as anthelmintic drugs provided to endothermic hosts. These interventions might impact T_{opt} differently and thus transmission phenology in areas where *S. mansoni* is endemic.

The objectives of this study were to: 1) quantify temperature-dependent *S. mansoni* and *Biomphalaria* spp. traits; 2) derive temperature-specific R_0 (i.e., estimated number of secondary cases from one infected human) predictions and thus a T_{opt} for schistosome transmission; 3) evaluate how R_0 and T_{opt} are affected by three interventions targeting distinct components of the parasite life cycle; and 4) explore the effects of temperature and interventions

Significance

Temperature influences the transmission of many pathogens, but the effects of temperature variability on parasite and host traits and their interactive effects on transmission are poorly understood. We integrated an epidemiological model of schistosomiasis, an infectious disease that affects over 200 million people, with temperature-dependent traits of the causative parasite and its intermediate snail host. We show that simulated interventions targeting snails and parasite larvae increased the optimum temperature for transmission because intervention-related mortality overrode natural thermal constraints. We show that interventions are more effective at lower temperatures, climate change will increase schistosomiasis risk in regions where surface water temperatures move closer to the thermal optimum, and considering local climate conditions for disease control can maximize human health outcomes.

Fig. 1. The schistosomiasis transmission cycle spans the endothermic human body and aquatic environment. Parameters representing temperature-dependent traits investigated in this study are highlighted in purple. Parameters pertaining to disease control interventions are highlighted in orange. Parameter definitions are given in the main text and *SI Appendix*, Table S6.

on transmission with regard to spatial and temporal surface water temperature variation.

We predicted that 1) parasite and snail traits would exhibit unimodal responses to temperature, allowing for the identification of a T_{opt} for each trait; 2) transmission (i.e., R_0) would decrease in response to all interventions; 3) T_{opt} of R_0 would only change in response to interventions targeting ectothermic parasite and host life stages; and 4) this in turn would alter transmission phenology in geographically and temporally dependent manners based on the proximity of local conditions to T_{opt}.

Results

Temperature-Dependent Life History Traits. We synthesized our experimental data and previously published data collected at constant temperatures to derive thermal response curves of life history traits of miracidia, cercariae, and snails. We found that miracidial hatching rate (γ_1) exhibited a linear response to temperature up to 37 °C (Fig. 2*A* and *SI Appendix*, Fig. S1*A*). A regression model with a linear temperature effect estimated that for each increase in temperature by 1 °C, the expected hatching success increased by ~4% (odds ratio for hatching success of 1.038, 95% CI 1.031–1.045). In contrast to the monotonic increase in miracidial hatching success with increasing temperature, we found that cercarial emergence (γ_2) showed a unimodal convex response to temperature (Fig. 2*B* and *SI Appendix*, Fig. S1*B*). The expected number of emerging cercariae peaked at 25.9 °C (95% CI 24.4, 27.7) at a rate of 306 (95% CI 240, 376) cercariae per snail per hour.

Estimated snail recruitment (Λ_2) showed a unimodal convex response to temperature and peaked at 22.1 °C (95% CI 21.5, 22.6) (Fig. 2*D*). Natural snail mortality (μ_2; Fig. 2*E*), miracidial mortality (μ_3; Fig. 2*F*), and cercarial mortality (μ_4; Fig. 2*G* and *SI Appendix*, Fig. S2) showed a unimodal concave response to temperature, with the lowest mortality rates occurring between 13 °C and 20 °C for all three parameters (*SI Appendix*, Table S4). Information about snail mortality due to infection (δ_2; Fig. 2*H* and *SI Appendix*, Fig. S3) and snail infectivity (β_2; Fig. 2*I*) was available for temperatures above ~20 °C only. We therefore were not able to fit a unimodal temperature response curve for either trait, but were limited to estimating logit-linear and log-linear temperature responses, respectively.

Diel temperature variation can influence transmission dynamics in host–parasite systems (24, 25). We found only one previous study examining the effects of diel variation in the schistosomiasis system, and the results showed no effect on parasite development

times in the snail host unless the daily minimum temperature dropped below 14 °C (26). To examine if other key snail and parasite life history traits were sensitive to diel temperature variation, we conducted an 11-wk experiment to measure snail egg production, snail growth, and cercarial emergence under both constant and five variable daily temperature regimes centered around an average temperature of 25.1 °C and a daily temperature range (DTR) between 1.9 °C and 30.5 °C. For snail egg production, infected snails exposed to an extreme DTR for water bodies inhabited by the parasite and its intermediate snail host (27–29) reproduced significantly less than infected snails exposed to constant temperature. Infected and uninfected snails exposed to the most extreme variable temperature regime, which greatly exceeded DTRs observed in the field (27–29), failed to reproduce. For snail growth and cercarial emergence, we found no significant difference between the constant and variable temperature treatments except for the most extreme variable temperature regime (*SI Appendix*, Fig. S4 and Table S5), suggesting that thermal response curves derived from constant temperatures (Fig. 2) are a reasonable estimate for trait responses in the field.

Effects of Temperature and Interventions on R_0 for Schistosomiasis. Using the thermal response curves derived from constant temperatures, we parameterized a mathematical model of schistosomiasis transmission dynamics (22) (*SI Appendix*, Fig. S5). We used this model to simulate temperature-dependent transmission risk (R_0) without any epidemiological intervention ("no control") and with the independent application of three interventions that targeted distinct parts of the parasite life cycle: 1) anthelminthic drug administration ("human treatment"), 2) snail control, and 3) cercarial control. Here, we use the term "control" to encompass the numerous approaches to reduce snail populations (e.g., molluscicide application, snail removal, snail habitat removal) or cercariae (e.g., water sanitation). We present relative R_0 values to focus on the effect of temperature-dependent parameters and interventions on transmission dynamics. Realized infection dynamics will be further determined by biological and socioeconomic factors, which we assumed to be temperature-invariant in the model (*SI Appendix*, Table S6).

In the no control and human treatment scenarios, R_0 peaked at 21.7 °C (95% CI 20.5, 23.1). Anthelminthic drug administration decreased human risk of infection by nearly an order of magnitude compared to no control measures (Fig. 3*A*). Out of the three interventions, snail control had the strongest effect on R_0, decreasing it by over 95% (Fig. 3*B*). As expected, human treatment had no effect on T_{opt} for transmission (Fig. 3*C*). In contrast, even low levels
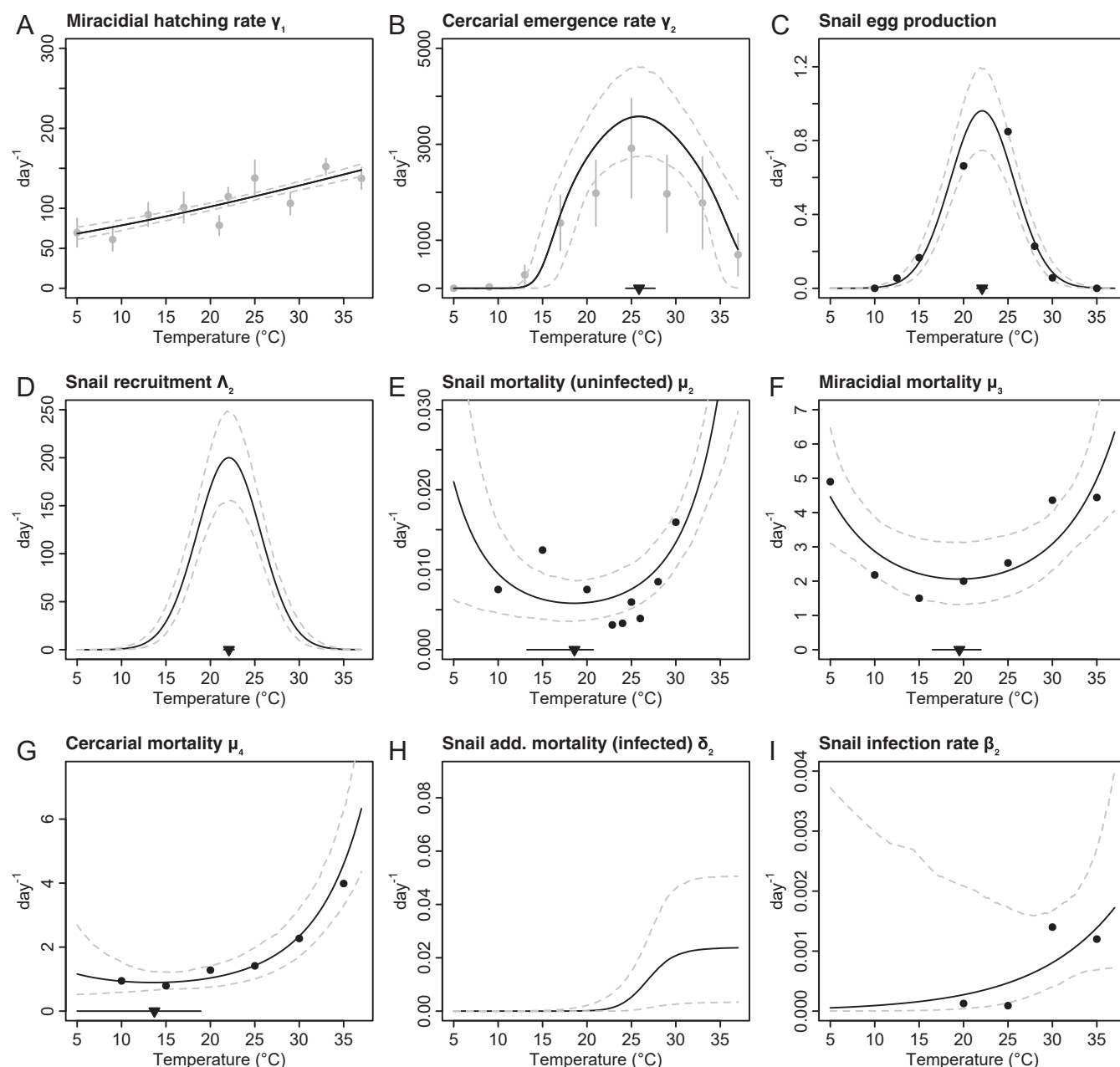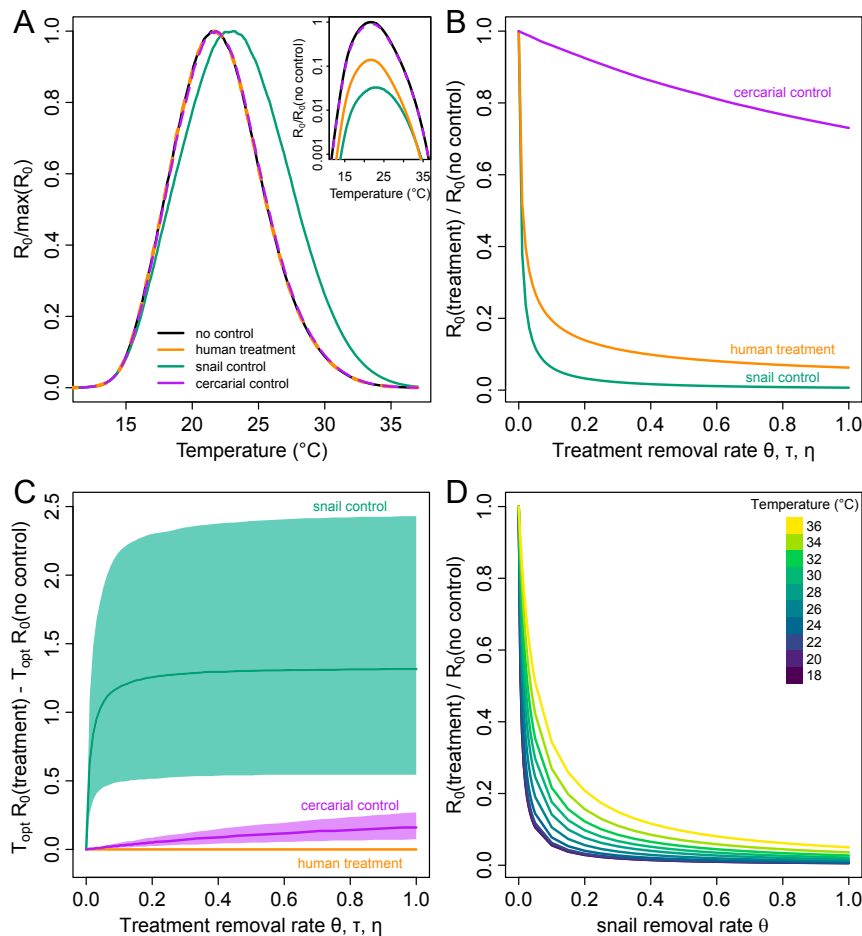
Fig. 2. Temperature dependence of life history traits of *S. mansoni* larval stages and snails. Thermal performance curves (posterior median and 95% credible intervals) were estimated from experiments conducted in this study (gray circles) (*A* and *B*) or from previously published data (black circles) (*C*–*I*). Data sources are given in the main text. Downward pointing triangles indicate the posterior estimate of T_{opt} (median and 95% CI) where applicable. (*C* and *D*) The temperature dependence of snail recruitment (Λ_2) was derived from egg production data. (*H*) Additional snail mortality due to infection (δ_2) was estimated from paired survival data (*SI Appendix*, Fig. S3). Full details of data sources and parameter estimation can be found in *SI Appendix*.

(<5%) of additional snail mortality from snail control rapidly increased the T_{opt} for transmission in a nonlinear fashion, as treatment mortality outpaced the temperature constraints on natural snail mortality, resulting in a T_{opt} shift of up to 1.32 °C (95% CI 0.54, 2.43) (Fig. 3*C* and *SI Appendix*, Fig. S6). Cercarial control also induced a small, but statistically significant, upward shift of T_{opt} by up to 0.16 °C (95% CI 0.08, 0.27) (Fig. 3*C* and *SI Appendix*, Fig. S6). We conducted additional sensitivity analyses to 1) determine whether variation in temperature-invariant model parameters would impact the observed shift of T_{opt} under snail and cercarial control scenarios and 2) assess the effects of nonlinear averaging of the R_0 projections across simulated diel temperature variations

(30). Even though absolute R_0 varied by as much as an order of magnitude depending on the values of temperature-invariant input parameters, our main finding that snail and cercarial control can shift the T_{opt} of R_0 remained robust to these changes (*SI Appendix*, Fig. S7). The shift of T_{opt} under snail and cercarial control scenarios persisted when simulating diel temperature variations similar to those observed in the field (28), although diel temperature ranges >6 °C resulted in an attenuation of the T_{opt} shift (*SI Appendix*, Fig. S8).

Given the profound effect of snail control on transmission risk and the T_{opt} for transmission, we further investigated the impact of snail control on R_0 at temperatures ranging from 18 °C to

Nguyen et al.
Interventions can shift the thermal optimum for parasitic disease transmission

PNAS | 3 of 8
https://doi.org/10.1073/pnas.2017537118

Fig. 3. Interventions and temperature-dependent life history traits shape schistosomiasis transmission risk. (*A*) Posterior predictions of the temperature dependence of R_0 based on temperature-dependent life history traits derived in this study. R_0 curves are scaled to the maximum R_0 of each scenario and are shown for transmission with no control (black) and three interventions targeting distinct parts of the life cycle at a 20% removal rate: human anthelminthic drug administration (orange), snail control (green), and cercarial control (purple). (*B*) All treatments reduced absolute transmission risk, with snail control having the strongest effect on reducing R_0. Curves show the ratio of R_0 under treatment and R_0 in the absence of control measures. (*C*) The T_{opt} at which the maximum transmission rate R_0 occurs is dependent on different intervention methods and intensities. Ninety-five percent credible intervals incorporate the uncertainty about individual temperature–trait relationships. Snail control (green) has the largest effect, shifting the T_{opt} of R_0 by as much as 1.32 °C (95% CI 0.54, 2.43). (*D*) Snail control at lower environmental temperatures is predicted to result in steeper reductions of R_0.

36 °C. We found that snail control was more effective at decreasing R_0 at cooler temperatures than at warmer temperatures (Fig. 3*D*).

Effects of Snail Control and Global Climate Change on the Seasonality of Schistosomiasis. The thermal constraints on T_{opt} and its increase in response to snail control measures revealed by our model suggested that regional surface water climatologies, global climate change, and interventions targeting snail populations should shape seasonal schistosomiasis dynamics. To explore the interplay of temperature-driven ecophysiological constraints on transmission and snail control, we used in situ water temperature data from a study conducted in Burkina Faso (31) to generate monthly R_0 predictions with and without snail control.
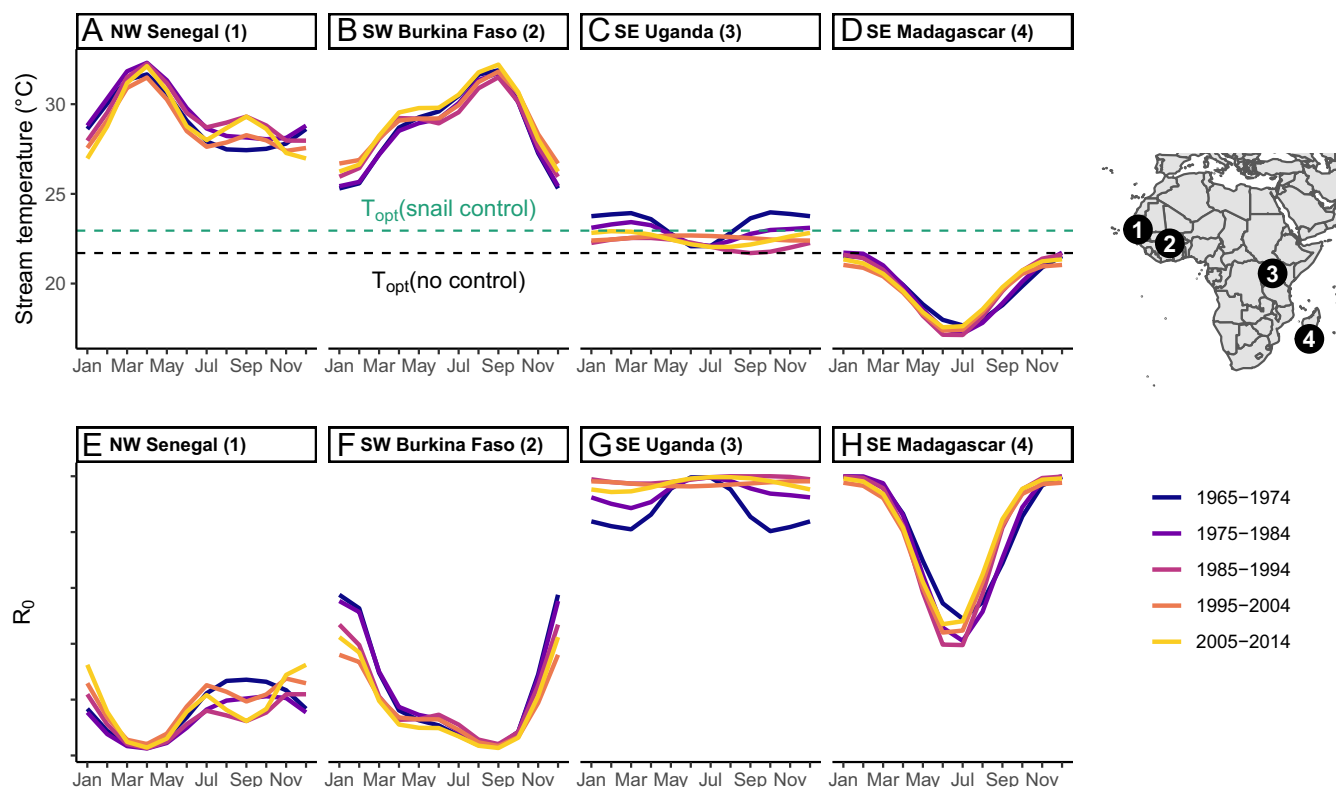
Average surface water temperatures were closer to the T_{opt} for transmission from November through March than in the remainder of the year (*SI Appendix*, Fig. S9A). This resulted in a peak in R_0 during cooler months and a decrease in R_0 during warmer months (*SI Appendix*, Fig. S9B). Snail control decreased R_0 throughout the year, but compared to the marked effect of seasonal temperature variation on R_0, the effect of snail control on R_0 seasonality was more subtle. Snail control decreased the effect of

seasonal differences in R_0 and broadened the seasonal R_0 peak during winter months (*SI Appendix*, Fig. S9C).

Detailed in situ surface water climatologies are rare across the range of *S. mansoni*, and future predictions of surface water temperatures under climate change are not widely available (32, 33). We therefore used monthly mean surface water temperatures from a retrospective global stream temperature model (34) to project R_0 phenologies from 1965 to 2014 for four areas endemic with schistosomiasis, representing arid (northwest Senegal), semiarid (southwest Burkina Faso), tropical (southeast Uganda), and subtropical climates (southeast Madagascar), respectively (Fig. 4 *A–D*).

Seasonal R_0 peaks occurred when surface water temperatures approached the T_{opt} for transmission, which occurred in boreal winter for sites north of the equator (Fig. 4 *E* and *F*), but in austral summer for the Madagascar site, which is south of the equator (Fig. 4*H*). Decadal variation in surface water temperatures since 1965 was small compared to the seasonal and regional temperature variation, but nonetheless led to changes in the projected R_0 phenologies. In Senegal, warmer autumns and colder winter conditions led to a shift in the seasonal R_0 maximum from autumn to winter (Fig. 4*E*), while warmer winters in Burkina Faso led to a

Fig. 4. Decadal and seasonal surface water temperature variation shapes regional transmission phenology. (A–D) Decadal averages of seasonal stream temperature dynamics across the range of *S. mansoni* in Africa based on Wanders et al. (34). (E and F) Decadal R_0 projections show the effect of spatial and temporal climate variability on schistosomiasis infection risk. Sites with water temperatures above T_{opt} (E, 1 and F, 2) have an inverted R_0 phenology compared to sites with water temperatures below T_{opt} (H, 4). The effect of decadal temperature variation is most pronounced at the equatorial site (G, 3). Note, the *y* axis for R_0 is not scaled because its absolute value at a given locality depends on biological and socioeconomic factors outside the scope of this study.

reduced winter peak of transmission risk (Fig. 4F). In Uganda, seasonal differences in surface water temperatures had diminished, leading to a year-round near-constant transmission risk in more recent years (Fig. 4G), and lower austral winter temperatures in the subtropical locality led to a reduction of the annual transmission risk minimum (Fig. 4H). Generally, our results suggest that surface water warming associated with global climate change will likely decrease infection risk in areas with surface water temperatures currently above the T_{opt} for transmission and increase infection risk in areas with surface water temperatures currently below the T_{opt} for transmission.

Snail removal reduced the absolute magnitude of R_0 under all climatic conditions, but its effect on transmission risk phenologies was more subtle. In regions where surface water temperatures were generally above the T_{opt} for transmission, seasonal differences in transmission risk were reduced, whereas seasonal differences became more pronounced under snail removal in regions where temperatures were colder than T_{opt} (*SI Appendix*, Fig. S10).

Discussion

Evaluating and increasing the effectiveness of control measures for parasitic diseases is predicated on understanding the temperature dependence of parasites and host life cycles across an ecologically relevant temperature gradient (35). In this study, we investigated the temperature sensitivity of life history traits of miracidia, cercariae, and snails to refine an existing epidemiological model of schistosomiasis. The inclusion of temperature-dependent life history traits yielded a temperature-dependent estimate of the basic reproductive number R_0, the expected number

of secondary infections given an infected human. In the absence of control measures, R_0 was predicted to be highest at 21.7 °C (95% CI 20.5, 23.1). All interventions decreased R_0, but snail control decreased R_0 by over 95% and shifted the optimum temperature (T_{opt}) of R_0 by as much as 1.32 °C (95% CI 0.54, 2.43; Fig. 3C). These effects were robust to variation in biological and socioeconomic factors (*SI Appendix*, Fig. S7) and simulated diel temperature variation (*SI Appendix*, Fig. S8). Additionally, we found that snail control was more effective at decreasing R_0 at cooler temperatures (Fig. 3D), which can inform seasonal intervention strategies in the field (*SI Appendix*, Figs. S9 and S10). When we projected R_0 values for climatically distinct areas across the *S. mansoni* range in Africa, regions with surface water temperatures colder than the T_{opt} for schistosomiasis had an inverted transmission risk phenology compared to areas with surface water temperatures warmer than T_{opt}. Together, these findings show that ecophysiological constraints and interventions can shape seasonal transmission dynamics. Predicting the influence of future climate change on surface water temperatures, and thus aquatic parasite transmission risk, is challenging as surface water temperatures arise from the interplay of precipitation and atmospheric and aquatic heat budgets (32–34), and to date no high-resolution projections of surface water temperatures under climate change are available for areas endemic with schistosomiasis. However, our projections based on past surface water temperature variability highlight that global climate change will lead to distinct regional changes in schistosomiasis transmission risk as environmental conditions in each area move closer to or further from the T_{opt} for transmission, respectively. Thus, interventions that target temperature-dependent life stages when seasonal temperatures are near the T_{opt} for transmission may

Nguyen et al.
Interventions can shift the thermal optimum for parasitic disease transmission

PNAS | 5 of 8
https://doi.org/10.1073/pnas.2017537118

ECOLOGY

achieve larger reductions in transmission risk than when temperatures are far from the T_{opt}.

Implications of Temperature and Interventions on R_0 for Schistosomiasis. By determining temperature-dependent life history traits from experimental and published data, we demonstrated that human risk of infection (R_0) is temperature-sensitive and peaks at 21.7 °C in the absence of control measures (Fig. 3A). We expected a T_{opt} for R_0 closer to the T_{opt} values for miracidial hatching and cercarial emergence, which were beyond 37 °C and at 25.9 °C, respectively (Fig. 2 A and B). However, the minimum mortalities for snails, miracidia, and cercariae peaked at 18.6 °C, 19.5 °C, and 13.7 °C, respectively (Fig. 2 E–G and *SI Appendix*, Table S4), which likely drove T_{opt} for R_0 downward toward cooler temperatures relative to the warmer T_{opt} values for hatching success and cercarial emergence. Our findings echo those of Mordecai et al. (3), who found that the inclusion of nonlinear thermal responses of mosquito and parasite life history traits predicted a T_{opt} for malaria 6 °C lower than previously predicted, and highlight how trait-based approaches can predict the temperature dependence of transmission across many host–parasite and vector–parasite systems (1, 36, 37).

Simulating human anthelminthic drug administration (human treatment), snail control, and cercarial control showed that human risk of infection varied depending on the target of the control measure. Our model revealed that all three interventions reduced R_0, with the strongest effect resulting from snail control, followed by human treatment, and then direct reductions of cercariae (Fig. 3 A and B).

Targeting intermediate snail hosts significantly impacts disease dynamics because snails are relatively long-lived and can produce cercariae daily, and additional mortality from snail control is markedly larger than the natural mortality rates of infected and uninfected snails. Applying temperature-explicit trait data led us to the discovery that snail control shifts the T_{opt} for R_0 by as much as 1.32 °C. Under natural conditions, snail mortality is low compared to the mortalities of the free-living larval stages (i.e., miracidia and cercariae). At temperatures above ~30 °C, snail mortality rapidly increases to almost 10-fold higher than the minimum snail mortality experienced at T_{opt} (Fig. 2E and *SI Appendix*, Fig. S6). In the absence of control measures, the steep increase in snail mortality constrains transmission at warm temperatures. The effect of snail control on T_{opt} arises because the additional mortality from snail control dwarfs natural snail mortality rates even at daily removal rates of <5%. This in turn diminishes the relative importance of the temperature dependence of natural and infection-related snail mortality on the overall mortality rates (*SI Appendix*, Fig. S6) and allows the overall T_{opt} of transmission to occur at higher temperatures (albeit at a reduced magnitude) (Fig. 3 A and B).

Conversely, removing cercariae does not greatly impact disease dynamics because these free-living larval stages have naturally high mortality rates. That is, the relative temperature response of cercarial mortality is only weakly affected by increased cercarial mortality rates due to control measures (*SI Appendix*, Fig. S6). When we simulated human treatment with anthelminthic drugs, the magnitude of R_0 decreased (Fig. 3A), but T_{opt} remained the same. This result was unsurprising as the probability of transmission per cercarial contact and parameters related to life history processes within the homeothermic environment of the human body were kept temperature-invariant in our model (Fig. 1 and *SI Appendix*, Fig. S5 and Table S6). Overall, our model supports both theoretical and experimental work showing that snail control decreases schistosomiasis transmission risk and that focusing on human treatment alone will not likely lead to eradication (38–41).

Applications of Our Model to Improve Disease Control. Transmission dynamics for many host–parasite and host–vector systems are driven by temperature (42–44) and, more specifically, by seasonal and diel temperature fluctuations (28, 42, 45). Agricultural demands, land use changes, human population growth, local thermal adaption, behavioral plasticity of parasite and hosts, and climate-driven phenological shifts between pathogens, vectors, and hosts can further influence transmission dynamics (32, 46–50). Together, these aspects can shape absolute transmission risk and seasonal transmission dynamics.

Our study highlights how trait-based approaches can identify ecophysiological constraints that influence human transmission risk (R_0) and the potential impacts of interventions on host–parasite interactions. As stated previously, diel temperature fluctuations can greatly influence key factors related to disease transmission involving ectothermic vectors or pathogens (24, 25). DTRs in water bodies likely to be inhabited by *S. mansoni* and *Biomphalaria* spp. range from 0 °C to 10 °C (27–29). Although the effect of such short-term fluctuations on traits of the parasite and its intermediate snail host are poorly understood, we were able to demonstrate that several key traits are unaffected by diurnal variations at temperatures near the T_{opt} of R_0, except when experimental DTRs were extreme or greatly exceeded those observed in the field (27–29) (*SI Appendix*, Fig. S4 and Table S5). This is in agreement with previous findings that development times of the parasite in its intermediate snail host are similar to those at equivalent constant average temperatures unless the daily temperature minimum drops below 14 °C (26). We further explored potential effects of diel temperature variations by averaging R_0 projections over a simulated diel temperature cycle and found that the observed shift of T_{opt} of R_0 held qualitatively (*SI Appendix*, Fig. S8 C and D). While this approach makes strong biological assumptions (i.e., no latency, acclimatization effects, or other physiological adjustments related to previous short-term exposures to temperature extremes), it did demonstrate that our findings are robust to the effects of nonlinear averaging of the R_0 projections (30) on realistic DTRs in the core endemic range of schistosomiasis. Our assumptions are less likely to hold at the thermal extremes of the schistosomiasis range, so there is a need to better understand both the DTRs of water bodies across the range of this disease, as well as the responses of the parasite and snail host to them (32). Despite these limitations, our findings outline the fundamental physiological niche of the transmission cycle and provide a baseline for future empirical work on site-specific parameters related to regional surface water temperature fluctuations and host behavior (e.g., those that mediate contact rates between miracidia and snails or cercariae and humans).

Overall, our study demonstrates that R_0 is sensitive to temperature-dependent life history traits of a parasite and its intermediate snail host and that including temperature-dependent parameters have knock-on effects on disease dynamics under different climatic conditions and intervention scenarios. Our results suggest that the efficacy of control measures for host–parasite systems may depend on whether an intervention method shifts the T_{opt} for transmission closer to or farther away from the natural temperature range of the area, which would increase or decrease disease transmission, respectively. Future disease models should account for how control strategies alter the T_{opt} for transmission of vector-borne diseases or diseases with environmental parasitic stages to improve human health outcomes in the context of a changing climate.

Materials and Methods

Estimating Temperature-Dependent Life History Traits. We conducted laboratory experiments to measure miracidial hatching success and cercarial emergence rates of *S. mansoni* at nine temperature treatments (5 °C, 9 °C, 13 °C, 17 °C, 21 °C, 25 °C, 29 °C, 33 °C, and 37 °C). Miracidial hatching success was determined visually from batches of eggs harvested from the livers of Swiss Webster mice exposed to the Naval Medical Research Institute (NMRI) strain of *S. mansoni* following a 24-h incubation period at the treatment temperature ($n = 216$). Cercarial emergence experiments were conducted with laboratory-reared *Biomphalaria glabrata* (NMRI strain) exposed to *S. mansoni* miracidia. Eight weeks post exposure, individual snails ($n = 72$) were acclimatized to treatment conditions for five days before undergoing emergence trials. Emerged cercariae were

stained with Lugol's iodine solution and counted (see *SI Appendix, Materials and Methods* for more details).

We estimated the temperature dependence of life history traits by fitting regression models to our experimental data and data from the literature. We specifically searched for experiments that examined the effect of temperature on survival and infectivity of *S. mansoni* and *Biomphalaria* spp., the intermediate snail host. We extracted data using Plot Digitizer 2.6.8. We determined uninfected and infected snail mortality rates from El-Hassan (20) and Foster (21), respectively; miracidial mortality rates from Anderson et al. (13); and cercarial mortality rates from Lawson and Wilson (15). We determined miracidial hatching rate (γ_1) by multiplying our experimental data with the average number of eggs produced per mated pair of schistosomes (51). We further used data from Mangal et al. (12) to derive temperature-dependent miracidial infection rates of snails. Snail egg production data from El-Hassan (20) was used to approximate the temperature dependence of snail recruitment. All thermal performance curves were determined from experiments conducted at constant temperature. Details of the parameter estimation can be found in *SI Appendix, Materials and Methods*.

To assess the effects of diurnal temperature variability on infection dynamics of *S. mansoni* and *B. glabrata*, we conducted an experiment that held mean temperature constant while manipulating diurnal temperature fluctuations and infection status for individual snail hosts. We established six treatments: a constant mean temperature (25.1 °C); a diurnal cycle with a DTR of 7.6 °C based on a 24-h temperature cycle measured at 10-min intervals in Asao Stream, near Kisumu, Kenya; and four treatments in which we multiplied the observed diurnal cycle by a factor to stretch or compress it while keeping it centered on the mean observed temperature. These multiplication factors were 0.25-, 0.5-, 2-, and 4-fold, resulting in DTRs of 1.9 °C, 3.9 °C, 15.3 °C, and 30.5 °C, respectively. The twofold treatment likely represents an extreme DTR for a water body inhabited by the parasite and its intermediate snail host, and the fourfold treatment greatly exceeds ecologically relevant field conditions (27–29). We tracked snail egg production, snail growth, and the production of schistosome cercariae over 11 wk. Each week, we counted the number of eggs laid per snail and measured the shell diameter of individual snails. Starting 4 wk post exposure, we also counted the number of emerged cercariae per snail and repeated this process for all surviving snails for 7 wk. Unexposed snails never released cercariae. We tested whether diurnal temperature variability affected final snail size, cumulative snail reproduction, and cumulative cercarial production using generalized linear models treating temperature regime and infection as interacting fixed categorical factors (see *SI Appendix, Materials and Methods* for more details).

Deriving R_0 for Schistosomiasis. We derived the basic reproductive number (R_0), the number of secondary cases from one infected human, based on a mathematical model of schistosomiasis transmission dynamics from Gao et al. (22) (Fig. 1 and *SI Appendix, Fig. S5*):

$$R_0 = \sqrt{\frac{\beta_1 \beta_2 \gamma \delta}{d_1 d_2 d_3 d_4 \mu_1 \mu_3}}. \quad \text{[1]}$$

Here, β_1 is the probability of human infection, β_2 is the probability of snail infection, γ describes the miracidial population, δ describes the cercarial population, d_1 is the death rate of infected humans, d_2 is the death rate of uninfected snails, d_3 is the death rate of infected snails, d_4 is the death rate of miracidia, μ_1 is the natural death rate of humans, and μ_3 is the natural death rate of miracidia. Additional equations were used to define γ, d_1, d_2, d_3, d_4, and δ and are as follows:

$$\gamma = \frac{k \Lambda_1 \gamma_1}{M_0} \quad \text{[2]}$$

$$d_1 = \mu_1 + \delta_1 + \eta \quad \text{[3]}$$

$$d_2 = \mu_2 + \theta \quad \text{[4]}$$

$$d_3 = \mu_2 + \delta_2 + \theta \quad \text{[5]}$$

$$d_4 = \mu_4 + \tau \quad \text{[6]}$$

$$\delta = \Lambda_2 \gamma_2. \quad \text{[7]}$$

Here, k is the portion of eggs leaving humans, Λ_1 is the recruitment rate of susceptible humans, γ_2 is the cercarial emergence rate, M_0 is the saturation coefficient for miracidial infectivity, μ_1 is the death rate of humans, δ_1 is the disease-related death rate of infected humans, η is the treatment rate of

infected humans, μ_2 is the death rate of uninfected snails, θ is the treatment elimination rate of snails, δ_2 is the disease-related snail mortality, μ_4 is the cercarial mortality rate, τ is the treatment elimination rate of cercariae, and Λ_2 is the recruitment rate of snails. Additional parameter details are given in *SI Appendix, Table S6*.

To derive temperature-dependent R_0 values, we used data from our miracidial hatching success (γ_1) and cercarial emergence (γ_2) trials and generated predictions for those parameters from 5 °C to 37 °C. Temperature-dependent predictions for μ_2, μ_3, μ_4, β_2, δ_2, and Λ_2 were derived from literature data (*SI Appendix, Materials and Methods*). Remaining parameters from the original model were kept constant with regard to temperature (*SI Appendix, Table S6*). Uncertainties in the estimated temperature dependencies of life history traits were propagated into the transmission risk model by generating R_0 predictions on random combinations of 1,000 posterior draws from each estimated thermal performance curve.

We evaluated the transmission risk model by simulating three intervention methods that targeted distinct parts of the parasite life cycle that were already modeled by Gao et al. (22): 1) anthelminthic drug administration (human treatment), 2) snail control, and 3) cercarial control. Each intervention was simulated independently with effective treatment removal rates of infected humans, snails, or cercariae, respectively, from 0 to 100% per day. We determined the optimal temperature of transmission (T_{opt}) and absolute transmission risk (R_0) for each treatment scenario. We generated posterior estimates of treatment effects on T_{opt} and R_0 based on paired comparisons of the treated and untreated R_0 model solutions for each of the 1,000 posterior draws.

Last, we investigated the sensitivity of R_0 projections and the effects of interventions to nonlinear averaging across simulated daily temperature variations (30). To achieve this aim, we solved Eq. 1 for hourly temperature estimates of a diel cycle based on realistic temperature observations (28) and the full range of simulated treatment mortalities of snails and cercariae described above. We then averaged the resulting hourly diel R_0 projections to generate an average daily R_0.

Projecting Seasonal R_0 Trajectories. We produced monthly R_0 projections for four areas endemic with schistosomiasis in Africa by matching temperature-specific R_0 estimates derived above to surface water temperature climatologies. We used monthly averages of in situ water temperature data for 2014–2015 from a site in Burkina Faso (31) to explore the combined effects of temperature and snail treatment (removal rate 0–50%) on R_0. To explore the impact of global climate change on schistosomiasis risk, we matched temperature-specific R_0 estimates to surface water temperatures from a retrospective global stream temperature model (34) for the period spanning 1965–2014. Retrospective R_0 phenologies were generated for the Burkina Faso location as well as three additional areas spanning the climatic gradient of where *S. mansoni* is endemic. These represent arid (northwest Senegal), semiarid (southwest Burkina Faso), tropical (southeast Uganda), and subtropical climates (southeast Madagascar). Smoothed monthly temperatures for each location and decade were derived using a generalized additive model. Details of the sites and data processing methods are given in *SI Appendix, Materials and Methods*.

Data Availability. Experimental and synthesized trait data have been deposited in Zenodo (https://doi.org/10.5281/zenodo.4494270) (52). Water temperature data from (31) are archived in the Knowledge Network for Biocomplexity Data Repository (DOI: 10.5063/F1F769HM) (53). Water temperature data from (34) are archived on Zenodo (DOI: 10.5281/zenodo.1468408) (54).

ECOLOGY

Nguyen et al.
Interventions can shift the thermal optimum for parasitic disease transmission

PNAS | 7 of 8
https://doi.org/10.1073/pnas.2017537118

1. E. A. Mordecai *et al.*, Thermal biology of mosquito-borne disease. *Ecol. Lett.* **22**, 1690–1708 (2019).

2. R. A. Taylor *et al.*, Predicting the fundamental thermal niche of crop pests and diseases in a changing world: A case study on citrus greening. *J. Appl. Ecol.* **56**, 2057–2068 (2019).

3. E. A. Mordecai *et al.*, Optimal temperature for malaria transmission is dramatically lower than previously predicted. *Ecol. Lett.* **16**, 22–30 (2013).

4. P. Coelho, R. L. Caldeira, Critical analysis of molluscicide application in schistosomiasis control programs in Brazil. *Infect. Dis. Poverty* **5**, 57 (2016).

5. D. Lowe *et al.*, Transport of *Schistosoma japonicum* cercariae and the feasibility of niclosamide for cercariae control. *Parasitol. Int.* **54**, 83–89 (2005).

6. L. Braun, J. E. T. Grimes, M. R. Templeton, The effectiveness of water treatment processes against schistosome cercariae: A systematic review. *PLoS Negl. Trop. Dis.* **12**, e0006364 (2018).

7. M. E. Woolhouse, On the application of mathematical models of schistosome transmission dynamics. II. Control. *Acta Trop.* **50**, 189–204 (1992).

8. N. C. Grassly, C. Fraser, Mathematical models of infectious disease transmission. *Nat. Rev. Microbiol.* **6**, 477–487 (2008).

9. A. F. Adenowo, B. E. Oyinloye, B. I. Ogunyinka, A. P. Kappo, Impact of human schistosomiasis in sub-Saharan Africa. *Braz. J. Infect. Dis.* **19**, 196–205 (2015).

10. D. G. Colley, A. L. Bustinduy, W. E. Secor, C. H. King, Human schistosomiasis. *Lancet* **383**, 2253–2264 (2014).

11. M. Pietrock, D. J. Marcogliese, Free-living endohelminth stages: At the mercy of environmental conditions. *Trends Parasitol.* **19**, 293–299 (2003).

12. T. D. Mangal, S. Paterson, A. Fenton, Predicting the impact of long-term temperature changes on the epidemiology and control of schistosomiasis: A mechanistic model. *PLoS One* **3**, e1438 (2008).

13. R. M. Anderson, J. G. Mercer, R. A. Wilson, N. P. Carter, Transmission of *Schistosoma mansoni* from man to snail: Experimental studies of miracidial survival and infectivity in relation to larval age, water temperature, host size and host age. *Parasitology* **85**, 339–360 (1982).

14. S. K. Prah, C. James, The influence of physical factors on the survival and infectivity of miracidia of *Schistosoma mansoni* and *S. haematobium* I. Effect of temperature and ultra-violet light. *J. Helminthol.* **51**, 73–85 (1977).

15. J. R. Lawson, R. A. Wilson, The survival of the cercariae of *Schistosoma mansoni* in relation to water temperature and glycogen utilization. *Parasitology* **81**, 337–348 (1980).

16. N. P. Carter, R. M. Anderson, R. A. Wilson, Transmission of *Schistosoma mansoni* from man to snail: Laboratory studies on the influence of snail and miracidial densities on transmission success. *Parasitology* **85**, 361–372 (1982).

17. J. C. Samuelson, J. J. Quinn, J. P. Caulfield, Hatching, chemokinesis, and transformation of miracidia of *Schistosoma mansoni*. *J. Parasitol.* **70**, 321–331 (1984).

18. B. Fried, R. LaTerra, Y. Kim, Emergence of cercariae of *Echinostoma caproni* and *Schistosoma mansoni* from *Biomphalaria glabrata* under different laboratory conditions. *J. Helminthol.* **76**, 369–371 (2002).

19. R. Poulin, Global warming and temperature-mediated increases in cercarial emergence in trematode parasites. *Parasitology* **132**, 143–151 (2006).

20. A. A. El-Hassan, Laboratory studies on the direct effect of temperature on *Bulinus truncatus* and *Biomphalaria alexandrina*, the snail intermediate hosts of schistosomes in Egypt. *Folia Parasitol. (Praha)* **21**, 181–187 (1974).

21. R. Foster, The effect of temperature on the development of *Schistosoma mansoni* Sambon, 1907 in the intermediate host. *J. Trop. Med. Hyg.* **67**, 289–292 (1964).

22. S. Gao, Y. Liu, Y. Luo, D. Xie, Control problems of a mathematical model for schistosomiasis transmission dynamics. *Nonlinear Dyn.* **63**, 503–512 (2010).

23. E. T. Chiyaka, W. Garira, Mathematical analysis of the transmission dynamics of schistosomiasis in the human-snail hosts. *J. Biol. Syst.* **17**, 397–423 (2011).

24. L. Lambrechts *et al.*, Impact of daily temperature fluctuations on dengue virus transmission by *Aedes aegypti*. *Proc. Natl. Acad. Sci. U.S.A.* **108**, 7460–7465 (2011).

25. K. P. Paaijmans *et al.*, Influence of climate on malaria transmission depends on daily temperature variation. *Proc. Natl. Acad. Sci. U.S.A.* **107**, 15135–15139 (2010).

26. W. Pflüger, Experimental epidemiology of schistosomiasis. II. Prepatency of *Schistosoma mansoni* in *Biomphalaria glabrata* at diurnally fluctuating temperatures. *Z. Parasitenkd.* **66**, 221–229 (1981).

27. A. F. Jacobs, B. G. Heusinkveld, A. Kraai, K. P. Paaijmans, Diurnal temperature fluctuations in an artificial small shallow water body. *Int. J. Biometeorol.* **52**, 271–280 (2008).

28. K. P. Paaijmans *et al.*, Observations and model estimates of diurnal water temperature dynamics in mosquito breeding sites in western Kenya. *Hydrol. Processes* **22**, 4789–4801 (2008).

29. J. O. Young, Seasonal and diurnal changes in the water temperature of a temperate pond (England) and a tropical pond (Kenya). *Hydrobiologia* **47**, 513–526 (1975).

30. M. Denny, The fallacy of the average: On the ubiquity, utility and continuing novelty of Jensen's inequality. *J. Exp. Biol.* **220**, 139–146 (2017).

31. J. Perez-Saez *et al.*, Hydrology and density feedbacks control the ecology of intermediate hosts of schistosomiasis across habitats in seasonal climates. *Proc. Natl. Acad. Sci. U.S.A.* **113**, 6427–6432 (2016).

32. N. McCreesh, M. Booth, Challenges in predicting the effects of climate change on *Schistosoma mansoni* and *Schistosoma haematobium* transmission potential. *Trends Parasitol.* **29**, 548–555 (2013).

33. I. Arismendi, M. Safeeq, J. B. Dunham, S. L. Johnson, Can air temperature be used to project influences of climate change on stream temperature? *Environ. Res. Lett.* **9**, 084015 (2014).

34. N. Wanders, M. T. H. Vliet, Y. Wada, M. F. P. Bierkens, L. P. H. Beek, High-resolution global water temperature modeling. *Water Resour. Res.* **55**, 2760–2778 (2019).

35. K. D. Glunt, J. I. Blanford, K. P. Paaijmans, Chemicals, climate, and control: Increasing the effectiveness of malaria vector control tools by considering relevant temperatures. *PLoS Pathog.* **9**, e1003602 (2013).

36. M. S. Shocket *et al.*, Temperature drives epidemics in a zooplankton-fungus disease system: A trait-driven approach points to transmission via host foraging. *Am. Nat.* **191**, 435–451 (2018).

37. B. A. Han, S. M. O'Regan, J. Paul Schmidt, J. M. Drake, Integrating data mining and transmission theory in the ecology of infectious diseases. *Ecol. Lett.* **23**, 1178–1188 (2020).

38. F. Allan *et al.*, Snail-related contributions from the schistosomiasis consortium for operational research and evaluation program including xenomonitoring, focal mollusciciding, biological control, and modeling. *Am. J. Trop. Med. Hyg.* **103**, 66–79 (2020).

39. C. H. King, L. J. Sutherland, D. Bertsch, Systematic review and meta-analysis of the impact of chemical-based mollusciciding for control of *Schistosoma mansoni* and *S. haematobium* transmission. *PLoS Negl. Trop. Dis.* **9**, e0004290 (2015).

40. S. H. Sokolow *et al.*, To reduce the global burden of human schistosomiasis, use 'old fashioned' snail control. *Trends Parasitol.* **34**, 23–40 (2018).

41. C. M. Hoover *et al.*, Modelled effects of prawn aquaculture on poverty alleviation and schistosomiasis control. *Nat. Sustain.* **2**, 611–620 (2020).

42. K. P. Paaijmans, A. F. Read, M. B. Thomas, Understanding the link between malaria risk and climate. *Proc. Natl. Acad. Sci. U.S.A.* **106**, 13844–13849 (2009).

43. R. Poulin, Meta-analysis of seasonal dynamics of parasite infections in aquatic ecosystems. *Int. J. Parasitol.* **50**, 501–510 (2020).

44. J. R. Rohr *et al.*, Frontiers in climate change-disease research. *Trends Ecol. Evol.* **26**, 270–277 (2011).

45. S. J. Kutz, E. P. Hoberg, L. Polley, E. J. Jenkins, Global warming is changing the dynamics of Arctic host-parasite systems. *Proc. Biol. Sci.* **272**, 2571–2576 (2005).

46. J. R. Rohr *et al.*, Emerging human infectious diseases and the links to global food production. *Nat. Sustain.* **2**, 445–456 (2019).

47. N. T. Halstead *et al.*, Agrochemicals increase risk of human schistosomiasis by supporting higher densities of intermediate hosts. *Nat. Commun.* **9**, 837 (2018).

48. J. M. Becker *et al.*, Pesticide pollution in freshwater paves the way for schistosomiasis transmission. *Sci. Rep.* **10**, 3650 (2020).

49. J. M. Cohen, M. J. Lajeunesse, J. R. Rohr, A global synthesis of animal phenological responses to climate change. *Nat. Clim. Chang.* **8**, 224–228 (2018).

50. E. D. Sternberg, M. B. Thomas, Local adaptation to temperature and the implications for vector-borne diseases. *Trends Parasitol.* **30**, 115–122 (2014).

51. C. Castillo-Chavez, Z. Feng, D. Xu, A schistosomiasis model with mating structure and time delay. *Math. Biosci.* **211**, 333–341 (2008).

52. K. H. Nguyen *et al.*, Trait data relating to the temperature-specific transmission of human schistosomiasis (Version v1.0). *Zenodo.* https://doi.org/10.5281/zenodo.4494270. Deposited 2 February 2021.

53. J. Perez-Saez *et al.*, Weekly counts of freshwater snails acting as interemediate hosts of schistosomiasis and habitat environmental data, Burkina Faso, 2014-2015. Knowledge Network for Biocomplexity. https://doi.org/10.5063/F1F769HM. Accessed 16 June 2020.

54. N. Wanders, M. van Vliet, Y. Wada, M. Bierkens, L. van Beek, Global monthly water temperature dataset, derived from dynamical 1-D water-energy routing model (DynWat) at 10 km spatial resolution (Version 1.0). *Zenodo.* http://doi.org/10.5281/zenodo.1468408. Accessed 22 May 2020.

Nguyen et al.
Interventions can shift the thermal optimum for parasitic disease transmission